NASA/TM—1998-208827 ARL–TR–1833

Three–Dimensional Gear Crack Propagation Studies

David G. Lewicki
U.S. Army Research Laboratory, Lewis Research Center, Cleveland, Ohio

Ashok D. Sane and Raymond J. Drago
Boeing Defense and Space Group, Philadelphia, Pennsylvania

Paul A. Wawrzynek
Cornell University, Ithaca, New York

DISTRIBUTION STATEMENT A
Approved for Public Release
Distribution Unlimited

19991004 251

December 1998

DTIC QUALITY INSPECTED 4

The NASA STI Program Office . . . in Profile

Since its founding, NASA has been dedicated to the advancement of aeronautics and space science. The NASA Scientific and Technical Information (STI) Program Office plays a key part in helping NASA maintain this important role.

The NASA STI Program Office is operated by Langley Research Center, the Lead Center for NASA's scientific and technical information. The NASA STI Program Office provides access to the NASA STI Database, the largest collection of aeronautical and space science STI in the world. The Program Office is also NASA's institutional mechanism for disseminating the results of its research and development activities. These results are published by NASA in the NASA STI Report Series, which includes the following report types:

- TECHNICAL PUBLICATION. Reports of completed research or a major significant phase of research that present the results of NASA programs and include extensive data or theoretical analysis. Includes compilations of significant scientific and technical data and information deemed to be of continuing reference value. NASA's counterpart of peer-reviewed formal professional papers but has less stringent limitations on manuscript length and extent of graphic presentations.

- TECHNICAL MEMORANDUM. Scientific and technical findings that are preliminary or of specialized interest, e.g., quick release reports, working papers, and bibliographies that contain minimal annotation. Does not contain extensive analysis.

- CONTRACTOR REPORT. Scientific and technical findings by NASA-sponsored contractors and grantees.

- CONFERENCE PUBLICATION. Collected papers from scientific and technical conferences, symposia, seminars, or other meetings sponsored or cosponsored by NASA.

- SPECIAL PUBLICATION. Scientific, technical, or historical information from NASA programs, projects, and missions, often concerned with subjects having substantial public interest.

- TECHNICAL TRANSLATION. English-language translations of foreign scientific and technical material pertinent to NASA's mission.

Specialized services that complement the STI Program Office's diverse offerings include creating custom thesauri, building customized data bases, organizing and publishing research results . . . even providing videos.

For more information about the NASA STI Program Office, see the following:

- Access the NASA STI Program Home Page at ***http://www.sti.nasa.gov***

- E-mail your question via the Internet to help@sti.nasa.gov

- Fax your question to the NASA Access Help Desk at (301) 621-0134

- Telephone the NASA Access Help Desk at (301) 621-0390

- Write to:
  NASA Access Help Desk
  NASA Center for AeroSpace Information
  7121 Standard Drive
  Hanover, MD 21076

NASA/TM—1998-208827 ARL–TR–1833

Three–Dimensional Gear Crack Propagation Studies

David G. Lewicki
U.S. Army Research Laboratory, Lewis Research Center, Cleveland, Ohio

Ashok D. Sane and Raymond J. Drago
Boeing Defense and Space Group, Philadelphia, Pennsylvania

Paul A. Wawrzynek
Cornell University, Ithaca, New York

Prepared for the Fourth World Congress on Gearing and Power Transmission
sponsored by the Institut des Engrenages et des Transmissions
Paris, France, March 16–18, 1999

National Aeronautics and
Space Administration

Lewis Research Center

December 1998

Available from

NASA Center for Aerospace Information
7121 Standard Drive
Hanover, MD 21076
Price Code: A03

National Technical Information Service
5285 Port Royal Road
Springfield, VA 22100
Price Code: A03

THREE-DIMENSIONAL GEAR CRACK PROPAGATION STUDIES

David G. Lewicki
U.S. Army Research Laboratory
Lewis Research Center
Cleveland, Ohio, 44135

Ashok D. Sane and Raymond J. Drago
Boeing Defense and Space Group
Philadelphia, Pennsylvania, 19142

Paul A. Wawrzynek
Cornell Fracture Group
Cornell University
Ithaca, New York, 14853

ABSTRACT

Three-dimensional crack growth simulation was performed on a split-tooth gear design using boundary element modeling and linear elastic fracture mechanics. Initial cracks in the fillet of the teeth produced stress intensity factors of greater magnitude (and thus, greater crack growth rates) than those in the root or groove areas of the teeth. Crack growth simulation was performed on a case study to evaluate crack propagation paths. Tooth fracture was predicted from the crack growth simulation for an initial crack in the tooth fillet region. Tooth loads on the uncracked mesh of the split-tooth design were up to five times greater than those on the cracked mesh if equal deflections of the cracked and uncracked teeth were considered. Predicted crack shapes as well as crack propagation life are presented based on calculated stress intensity factors, mixed-mode crack propagation trajectory theories, and fatigue crack growth theories.

INTRODUCTION

Gears used in current helicopters and turboprops are designed for light weight, high margins of safety, and high reliability. However, unexpected gear failures may occur even with adequate tooth design (Couchan, et al., 1993). In order to design an extremely safe system, the designer must ask and address the question "what happens when a failure occurs." With regards to gear tooth bending fatigue, tooth or rim fractures may occur. A crack which propagates through a rim would be catastrophic, leading to disengagement of a rotor or propeller, loss of an aircraft, and possible fatalities (McFadden, 1985, Albrecht, 1988). This failure mode should be avoided. A crack which propagates through a tooth itself may or may not be catastrophic, depending on the design and operating conditions. Also, early warning of this failure mode may be possible due to advances in modern diagnostic systems (Kershner, et al., 1997).

One concept proposed to address bending fatigue fracture from a safety aspect is a split-tooth gear design (Drago, et al., 1997). The prime objective of the split-tooth design is to control crack propagation in a desired direction such that at least half of the tooth remains operational should a bending failure occur. However, the split-tooth design should have the same weight, performance, and reliability characteristics as a conventional single-tooth design. Finite element models were developed to evaluate candidate split-tooth designs. These designs incorporated grooves through the center of the tooth face widths to 'split' the teeth. Stress, strength, durability, and sliding velocity studies were performed to demonstrate the feasibility of such a design.

The objective of the current study is to analytically validate the crack propagation failsafe characteristics of a split-tooth gear. A specially developed three-dimensional crack analysis program was used which was based on boundary element modeling and principles of linear elastic fracture mechanics. The effect of the location of initial cracks on crack propagation was evaluated. Crack growth simulation was performed on a case study to evaluate crack propagation paths. Predicted crack shapes as well as crack propagation life are presented based on calculated stress intensity factors, mixed-mode crack propagation trajectory theories, and fatigue crack growth theories.

I. ANALYSIS

A. Previous Finite Element Modeling

An initial study was conducted to determine the feasibility of a split-tooth design (Drago, et al., 1997). Here, analytical modeling was performed on a proposed grooved design for the sun gear of a commercial helicopter planetary system. The model was constructed and analyzed using commercial available finite element modeling tools (P3/Patran, 1993, MacNeal, 1981). The model was three dimensional and consisted primarily of 8-node hex elements with a limited number of 6-node wedge elements (fig. 1). The model had a total number of 24,248 elements and 30,900 nodes and used multipoint constraint boundary conditions to model the bearing supports. The mesh was refined for four of the teeth for improved stress prediction accuracy.

The purpose of the split-tooth design was to control crack propagation in a desired direction such that at least half of the gear face width remains operational should a failure occur. This was implemented by introducing a groove through the center of the face width of the existing configuration. In the initial Drago study, various groove widths and depths were analyzed to determine the optimized configuration. A detailed stress analysis of the tooth fillets and grooves was required to produce a strong gear, rim, web, and hub system for high-load helicopter applications. The study showed the feasibility of such a split-tooth design and subsequent experimental tests are planned for the future. The tests will use a single-tooth bending fatigue specimen and apparatus as described by Lemanski, et al. (1969). Due to this, the crack propagation studies in the current work will model the single-tooth bending fatigue test gear.

B. Model of the Single Tooth Bending Fatigue Gear

A split-tooth design was developed for future tests in a nonrotating single-tooth bending fatigue test fixture. The test fixture loads a tooth (or in this case, the two split teeth) on the test gear at the highest point of single tooth contact through a load anvil. The load anvil is connected to a universal fatigue machine which delivers a steady and alternating force. Load is transferred through the test gear and reacted by a reaction anvil at a location approximately 135° from the loaded tooth. The test gear has 32 teeth, 4.763 module (5.333 diametral pitch), 25° pressure angle, 15.24 cm (6.000 in.) pitch diameter, and 0.95 cm (0.375 in.) face width per tooth. A boundary element model of a split-tooth design of an uncracked single-tooth bending fatigue test gear is shown in figure 2. Note that four series of four successive teeth are removed from the test gear to allow installation in the test fixture. The complete gear, rim, and web assembly was modeled as well as removal of the appropriate teeth.

The mesh in the region of the loaded teeth (as well as the locations of the initial cracks) was refined for improved stress prediction accuracy. The model shown in figure 2 had 1816 elements (both 4-node quadrilateral and 3-node triangular) and 1479 nodes. The material properties used were that of steel (modulus of elasticity = 207 GPa (30×10^6 psi), Poisson's ratio = 0.3). An applied pressure along narrow patches on two split teeth at the location of the highest point of single tooth contact simulated a tooth load normal force of 24,541 N (5,517 lb) per tooth. Displacements on the reaction teeth as well as half of the inner hub diameter were constrained to zero to model the reaction anvil and hub support bearing.

C. Fracture Analysis Modeling Code

The Franc3d (Fracture Analysis Code for 3 Dimensions, Wawrzynek, 1991) computer code was used for crack simulation. This program was developed at Cornell University and an executable version is openly available to the public. Crack growth simulation is the main feature of the program. The program uses boundary element modeling and principles of linear elastic fracture mechanics to analyze cracked structures. The geometry of three-dimensional structures with nonplanar, arbitrary shaped cracks can be modeled. The simulation process is controlled by the user through a graphical user interface which includes windows for the display of the structure as well as a menu/dialog-box system for interacting with the program.

The modeling of a three-dimensional cracked structure is actually performed through a series of programs developed at Cornell University. First, the structure geometry grid point data is imported to a solid modeler program. Here, appropriate curves and faces (or patches) are created from the grid data as well as a closed-loop surface

geometry model. This surface model is then imported to the Franc3d program for boundary element model preparation. The user can then mesh the geometry model using 3 or 6 node triangular surface elements, or 4 or 8 node quadrilateral elements. Boundary conditions (applied tractions and prescribed displacements) are applied on the model geometry over faces, edges, or points. Initial cracks such as elliptical or penny shaped can be inserted in the structure. After complete formulation, the model is shipped to a boundary element equation solver program. Once the displacement and traction unknowns are solved, the results are exported back to the Franc3d program for post processing.

II. RESULTS AND DISCUSSION

A. Stress Analysis of an Uncracked Gear

The purpose of the stress analysis of an uncracked gear was: (1) to validate the mesh refinement for the loaded teeth, and (2) to compare the boundary element analysis results with previous Boeing Helicopter finite element analysis results. Previous studies have shown that accurate stress intensity factor predictions, and thus, accurate crack path predictions, were obtained if the initial mesh without a crack produced accurate estimates of the maximum stresses (Lewicki, 1995). The exaggerated deformation of an uncracked gear under load is shown in figure 3. As expected, the majority of the deflection was in the loaded teeth. The magnitude of the maximum deflection was 0.218 mm (0.0086 in.) at the tip of the loaded teeth. In addition, there was slight rotation about the gear rotational axis. Also, there was slight separation of the loaded teeth (best seen in the front view) and the deflection was symmetric with respect to the groove.

The element-averaged tooth fillet stress distribution is shown in figure 4. For these results, an equal pressure was applied to both the left and right teeth. However, the area of the applied load on the left tooth was about 1 percent greater than the right due to round off errors in the model formulation. Thus, the magnitude of the stresses on the left tooth was 1 percent greater than the right tooth. The maximum value of the maximum principle stress was 1213 MPa (176) ksi. This occurred on the left tooth at the center of the face width and at an angle approximately 40° with respect to the tooth centerline. As with the deflections, the stress distribution was symmetrical with respect to the groove. Finally, the overall stress distribution using the boundary element analysis was similar to that of the Boeing finite element model.

B. Effect of Initial Crack Location

The effect of the location of initial cracks on mode I stress intensity factors were analyzed for a variety of crack locations in the tooth fillet. Four initial cracks were analyzed, one at a time, with the same load and boundary conditions as previously described. Figure 5 shows the detailed boundary element mesh for initial crack 1. Figure 6 shows the mode I stress analysis factors for all four initial cracks. The stress intensity factors were determined as a function of position along the cracks front based on the calculated deflections using the method of Tracey (1977). All four initial cracks had the same shape, size, and orientation. They were all half-ellipse cracks with a width of 0.254 cm (0.100 in.), a depth of 0.127 cm (0.050 in.), and an orientation normal to the tooth fillet surface. Cracks 1 and 2 were on the left tooth biased toward the front and rear, respectively, while cracks 3 and 4 were on the right tooth biased toward the front and rear, respectively. For figure 6, the normalized position along the crack front starts with a value of zero at a position on the crack front toward the front of the tooth, then to a value of one following movement in the positive x-direction. The stress intensity factor versus position curves were similar for all four initial crack conditions. The stress intensity factors were greater near the ends of the crack front compared to the center. This indicated that the crack would grow along the tooth face width at a greater rate than through the tooth. In addition, based on the magnitude of the calculated stress intensity factors, a crack in a gear made of AISI 9310 steel material would grow in fatigue when subjected to the modeled geometry, load, and boundary conditions. This statement is based on data by Forman and Hu (1984), where they publish a stress intensity factor threshold of 3.2 MPa·$\sqrt{m}$ (3.5 ksi·$\sqrt{in.}$) and a fracture toughness value of 182 MPa·$\sqrt{m}$ (200 ksi·$\sqrt{in.}$) for AISI 9310 steel.

Figure 7 shows the effect of location for two initial root cracks on the right tooth. Crack 5 is in the center of the root at the forward edge of the face width while crack 6 is at the center of the face width. Crack 5 is a quarter-ellipse crack while crack 6 is a half-ellipse crack. As with the fillet initial cracks, crack 6 had a width of 0.254 cm

(0.100 in.) and a depth of 0.127 cm (0.050 in.). Again, an increase in the normalized crack front position followed movement in the positive x-direction. Crack 5 had a width of 0.127 cm (0.050 in.) and a depth of 0.127 cm (0.050 in.). Root crack 6 had a similar stress intensity factor distribution along the crack front as the fillet cracks of figure 6. However, the overall magnitudes were lower than the fillet cracks due to the decrease of the magnitude of the tensile stress field in the root compared to the fillet. Crack 5 had a greater stress intensity factor magnitude where the crack front intersected the tooth root compared to where the crack front intersected to side flank of the tooth. This also indicated that the crack would grow along the tooth width greater than it would tunnel through the tooth.

Figure 8 shows the effect of location for three initial cracks in the groove of the gear. Here an increase in the normalized position along the crack front follows movement in the positive z-direction. Initial crack 7 was about 0.08 cm (0.031 in.) below the root, crack 8 was about 0.037 cm (0.144 in.) below the root, and crack 9 was about 0.80 cm (0.315 in.) below the root. All three cracks had a width of 0.254 cm (0.100 in.), a depth of 0.127 cm (0.050 in.), and an orientation normal to the groove surface. The stress intensity factors were greatest for the crack nearest the fillet and root surface, again, since this was the location of the higher tensile stress field. The stress intensity factors decreased as the crack location was deeper into the tooth groove. Based on the magnitude of the mode I stress intensity factors, fatigue crack growth would still occur but at a rather low rate.

C. Propagation Path Study

The previously described initial crack 1 (fig. 5) was used for a crack growth simulation study. The procedure used to grow a crack was as follows. After initial crack 1 was inserted in the model, the mode I and mode II stress intensity factors were determined at 24 points along the crack front (mode I shown in fig. 6). The extended crack directions at these 24 points were determined using the ratio of mode II stress intensity factors to mode I and the mixed mode interaction theory of Erdogan and Sih (1963). The amount of crack extension at these points were determined based on the Paris crack growth relationship (Paris and Erdogen, 1963) where

$$a_i = a_{\max}\left(\frac{K_{I,i}}{K_{I,\max}}\right)^n$$

where a_i is the extension of the i_{th} point, $K_{I,i}$ is the mode I stress intensity factor of the i_{th} point, $K_{I,\max}$ is the value of the largest stress intensity factor along the crack front, $a_{\max}$ is the maximum crack extension which is specified by the user, and n is the Paris exponent. The maximum extension size, $a_{\max}$, was set at 0.13 cm (0.050 in.). The Paris exponent, n, was set at 2.954 based on material tests for AISI 9310 steel by Au and Ke (1981) and gear analysis and tests by Lewicki (1995). Using this procedure, a new crack front was produced with a nonplanar crack extension. A third-order polynomial was then used to model the extended crack front. The new crack geometry was then remeshed. After remeshing, the model was rerun and solved for displacements, stress intensity factors, and crack propagation directions. The above procedure was repeated a number of times to simulate crack growth in the gear tooth.

Figure 9 shows the extended crack geometry and mesh after two steps. Note that the maximum extension occurred at the trailing end of the crack front. At the leading end of the crack front, the crack extended to the tooth front flank. Figure 10 shows the extended crack after five calculation steps. By this time, the crack extended to the rear flank of the left tooth. After this, the crack propagated uniformly through the tooth face width. Figure 11 shows an exploded view of the tooth and crack after 15 propagation steps. As seen from the figure, the predicted failure is tooth fracture rather than rim fracture. From a failsafe aspect, this is the desired mode of failure.

With regards to tooth stiffness, the tooth compliance increased as the crack grew in size. This resulted in an increased deflection of the cracked tooth compared to the uncracked tooth for the same tooth load. This would probably not be the case during actual operation of a split-tooth design if one tooth of a driving gear was cracked and driving an uncracked driven gear. The mesh of the uncracked tooth would carry more load than the mesh of the cracked tooth. A contact analysis algorithm is needed to truly solve this complicated problem. The Franc3d software does not, unfortunately, have such an analysis capability and a manual approximation was used instead.

For each step during the crack growth simulation process, two runs at a given crack size were performed. The first was with equal applied loads on the cracked and uncracked tooth. The second was with adjusted loads to produced equal deflections for the cracked and uncracked teeth at a point on the tip of the loaded teeth at the center

of the face width. The second set of cases was accomplished through trial and error based on the trending of the equal loads case and adjusting the applied loads until the calculated deflections (from the boundary element analysis) of the crack and uncracked teeth were within 1 percent of each other.

Table I gives the results of the deflections and the loads from the analysis. After five steps (crack area of 0.263 cm^2 (0.041 $in.^2$)), the cracked-tooth deflection was 14 percent greater than the uncracked-tooth deflection for the same applied load on each. After 15 steps (crack area of 1.039 cm^2 (0.161 $in.^2$)), the cracked-tooth deflection was 220 percent greater than that of the uncracked tooth. Figure 12 depicts the applied load as a function of crack area for the constraint of equal tooth deflections. Note that at a crack area of 1.039 cm^2 (0.161 $in.^2$), the applied load on the uncracked tooth is almost five times that of the cracked tooth. This resulting overload on the uncracked tooth needs to be considered in the failsafe design of split-tooth configuration.

Finally, the predicted number of cycles during the crack growth simulation was estimated. The mode I stress intensity factors as a function of the crack front position for various steps are given in figure 13. The numbers on the curves correlate to the step number. Again, note the increase in the values of the stress intensity factors at the edges of the crack front for the initial steps. This implied that the crack grew in the tooth face width direction at a greater rate then through the tooth. At higher step sizes, the stress intensity factors where more uniform along the face width indicating uniform crack extension. The maximum value of the stress intensity factors along a given crack front for a given crack size is shown in figure 14 as a function of crack area. This was used in the Paris crack growth theory (Paris and Erdogen, 1963) where

$$\frac{da}{dN} = C\left(\Delta K_I\right)^n$$

where da is the crack extension distance for dN number of cycles, $C = 8.433 \cdot 10^{-9}$, and $n = 2.954$ for AISI 9310 steel material from Au and Ke (1981). Using the Paris theory, a typical life prediction for a cracked structure would exhibit an exponential decrease in the number of cycles as a crack would grow at a given applied load. This is due to the increase in the mode I stress intensity factor with crack size, and thus, decreased life. However, since the load on the uncracked tooth was adjusted for equal deflections (i.e., decreased as the crack grew in size), the stress intensity factors were nearly constant as the crack grew in size. This resulted in a rather linear increase in cycles with crack area after an initial growth at the start of the propagation simulation.

CONCLUSIONS

Three-dimensional crack growth simulation was performed on a split-tooth gear design using boundary element modeling and linear elastic fracture mechanics. The following conclusions were made: Initial cracks in the fillet of the teeth produced stress intensity factors of greater magnitude (and thus, greater crack growth rates) than those in the root or groove areas of the teeth. Tooth fracture was predicted from the crack growth simulation for an initial crack in the tooth fillet region. This was the desired failure mode for an ultra-safe design. Tooth loads on the uncracked mesh of the split-tooth design were up to five times greater than those on the cracked mesh if equal deflections of the cracked and uncracked teeth were considered. The effect of this needs to be considered in the design of a split-tooth configuration.

REFERENCES

Albrecht, C., 1988: "Transmission Design Using Finite Element Method Analysis Techniques," Journal of American Helicopter Society, Vol. 33, No. 2, Apr., pp. 3–14.

Au, J.J., and Ke, J.S., 1981: "Correlation Between Fatigue Crack Growth Rate and Fatigue Striation Spacing in AISI 9310 (AMS 6265) Steel," Fractography and Materials Science, ASTM STP 733, pp. 202–221.

Couchan, D.C., Barnes, G.K., and Cedoz, R.W., 1993: "Shot-Peened Gear Failures Due to Operation in a Misaligned Condition," AIAA Paper No. AIAA-93-2147, June.

Drago, R.J., Sane, A.D., and Brown, F.W., 1997: "UltraSafe Gear Systems for Critical Applications – Initial Development," AGMA TP–97FTM10, Nov.

Erdogan, F., and Sih, G.C., 1963: "On the Crack Extension in Plates Under Plane Loading and Transverse Shear," Journal of Basic Engineering, Vol. 85, pp. 519–527.

Forman, R.G., and Hu, T., 1984: "Application of Fracture Mechanics on the Space Shuttle," Damage Tolerance of Metallic Structures: Analysis Methods and Applications, ASTM STP 842, pp. 108–133.

Kershner, S., Johnson, J., and Gamauf, M., 1997: "Sikorsky Support to Commercial Health and Usage Monitoring Systems (HUMS): A Summary of Forty Months of Support," Proceedings of the AHS 53rd Forum, Virginia Beach, VA, pp. 1233–1241, Apr.

Lemanski, A.J., Alberti, J.P., and Rose, H.J., 1969: "Evaluation of Advanced Gear Materials for Gear Boxes and Transmissions," Report No. D210-10025-1, The Boeing Company, Vertol Division. Aug.

Lewicki, D.G., 1995: "Crack Propagation Studies to Determine Benign or Catastrophic Failure Modes for Aerospace Thin-Rim Gears," Ph.D. Dissertation, Case Western Reserve University, May.

MacNeal, R.H., 1981: "Handbook for Linear Static Analysis," MSC/NASTRAN, The MacNeal-Schwendler Corporation, Dec.

McFadden, P.D., 1985: "Analysis of the Vibration of the Input Bevel Pinion in RAN Wessex Helicopter Main Rotor Gearbox WAK143 Prior To Failure," Aeronautical Research Laboratories Report No. AR-004-049.

P3/PATRAN, 1993, P3/PATRAN User Manual, PDA Engineering, Costa Mesa, CA.

Paris, P.C., and Erdogen, F., 1963: "A Critical Analysis of Crack Propagation Laws," Journal of Basic Engineering, Vol. 85, pp. 528–534.

Tracey, D.M., 1977: "Discussion of 'On the Use of Isoparametric Finite Elements in Linear Fracture Mechanics' by R.S. Barsoum," International Journal for Numerical Methods in Engineering, Vol. 11, pp. 401–402.

Wawrzynek, P.A., 1991: "Discrete Modeling of Crack Propagation: Theoretical Aspects and Implementation Issues in Two and Three Dimensions," Ph.D. Dissertation, Cornell University.

TABLE I.—CALCULATED DEFLECTIONS FOR EQUAL LOADS AND LOADS FOR EQUAL DEFLECTIONS

Crack area, cm^2	Equal loads				Equal deflections				
	Load on each tooth, KN	Cracked tooth deflection, mm	Uncracked tooth deflection, mm	Difference in deflections, percent	Load on cracked tooth, KN	Cracked tooth deflection, mm	Load on uncracked tooth, KN	Uncracked tooth deflection, mm	Difference in deflections, percent
0.014	25,108	0.214	0.212	0.9	25,108	0.214	25,108	0.214	0.0
0.052	25,108	0.215	0.213	0.9	24,950	0.215	25,266	0.213	0.9
0.099	25,108	0.220	0.212	3.8	24,207	0.216	26,009	0.217	–0.5
0.131	25,108	0.224	0.212	5.7	24,009	0.218	26,207	0.217	0.5
0.165	25,108	0.228	0.212	7.5	23,788	0.221	26,428	0.218	1.4
0.263	25,108	0.242	0.212	14.2	22,473	0.227	27,743	0.225	0.9
0.298	25,108	0.249	0.212	17.5	21,730	0.229	28,486	0.229	0.0
0.356	25,108	0.261	0.213	22.5	20,758	0.233	29,458	0.234	–0.4
0.423	25,108	0.276	0.213	29.6	19,765	0.239	30,451	0.239	0.0
0.506	25,108	0.299	0.212	41.0	18,420	0.246	31,796	0.245	0.4
0.597	25,108	0.327	0.212	54.2	16,960	0.253	33,256	0.252	0.4
0.686	25,108	0.361	0.212	70.3	15,292	0.259	34,924	0.261	–0.8
0.768	25,108	0.402	0.211	90.5	13,884	0.266	36,332	0.268	–0.7
0.857	25,108	0.469	0.211	122.3	12,132	0.277	38,084	0.277	0.0
0.951	25,108	0.554	0.212	161.3	10,434	0.286	39,782	0.287	–0.3
1.039	25,108	0.680	0.212	220.8	8,621	0.294	41,595	0.297	–1.0

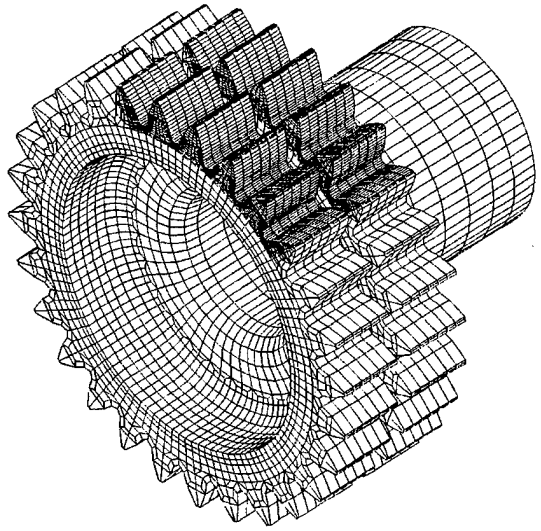

Figure 1. Finite element model of split-tooth gear configuration (Drago, et al., 1997).

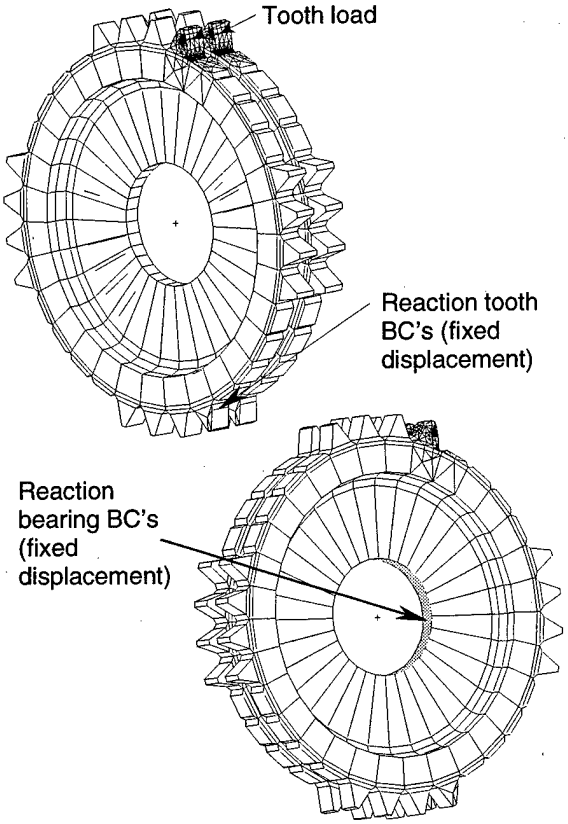

Figure 2. Boundary element model of a split-tooth bending fatigue test gear.

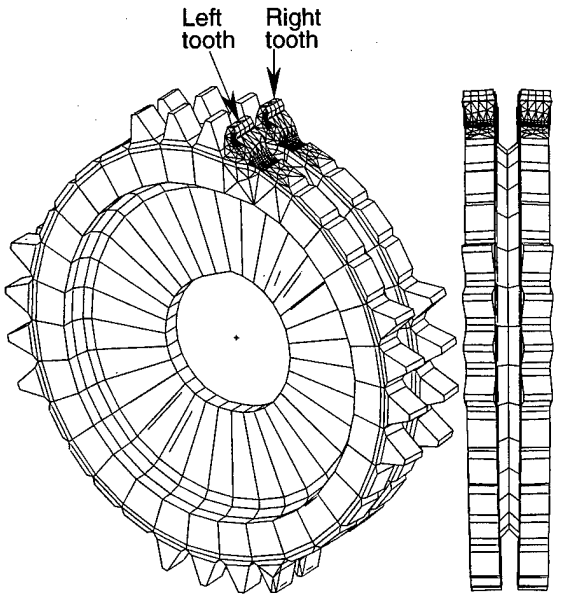

Figure 3. Boundary element model deflections of an uncracked split-tooth bending fatigue test gear.

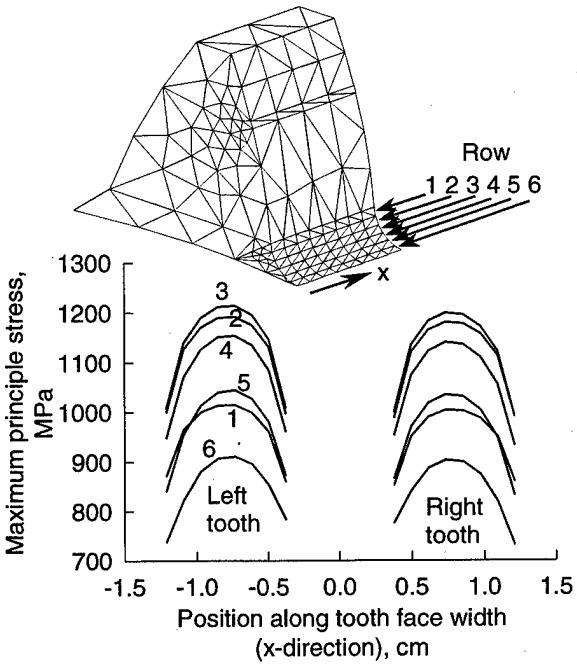

Figure 4. Fillet stresses from the boundary element model of an uncracked split-tooth bending fatigue test gear.

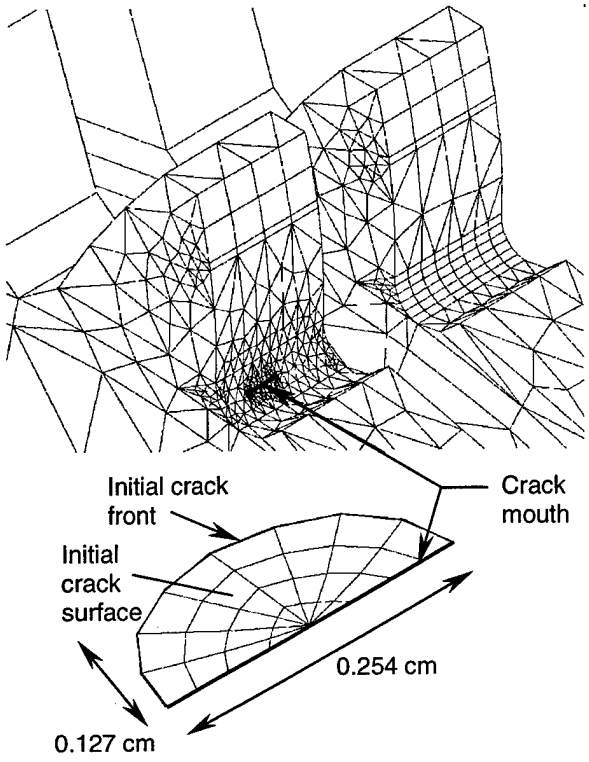

Figure 5. Boundary element mesh for initial crack 1.

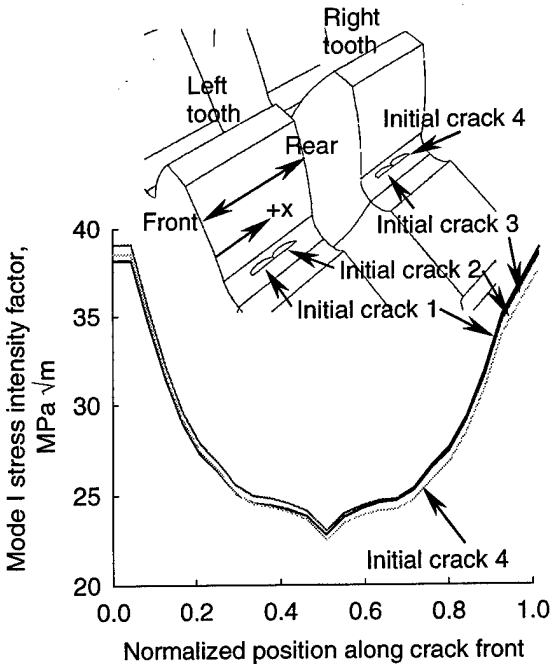

Figure 6. Effect of initial crack location on mode I stress intensity factors; tooth fillet locations.

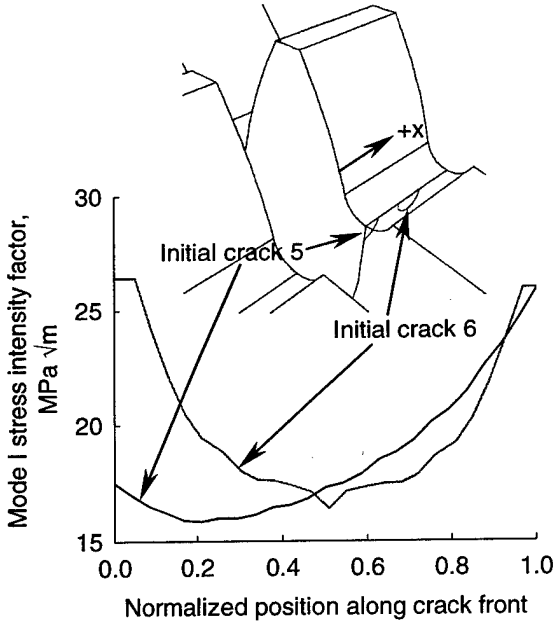

Figure 7. Effect of initial crack location on mode I stress intensity factors; tooth root locations.

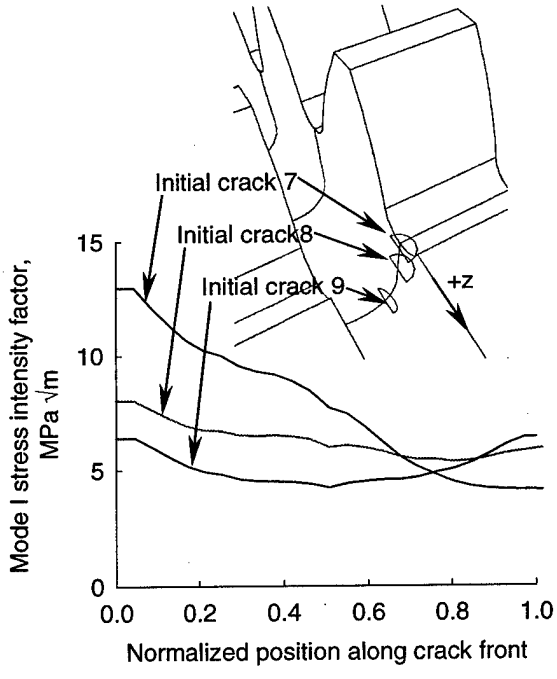

Figure 8. Effect of initial crack location on mode I stress intensity factors; tooth groove locations.

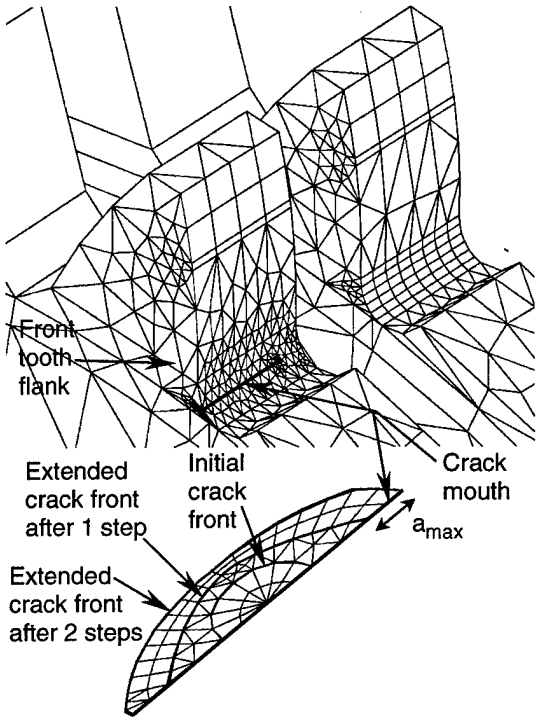

Figure 9. Predicted crack extension for initial crack 1 case study after two steps.

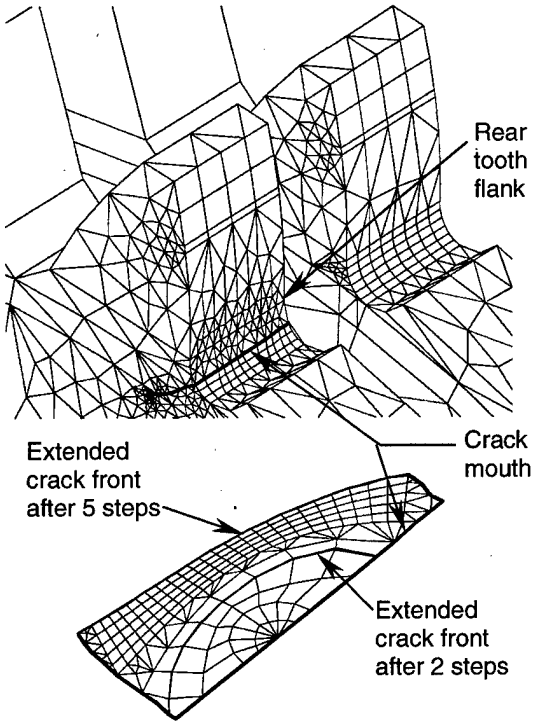

Figure 10. Predicted crack extension for initial crack 1 case study after five steps.

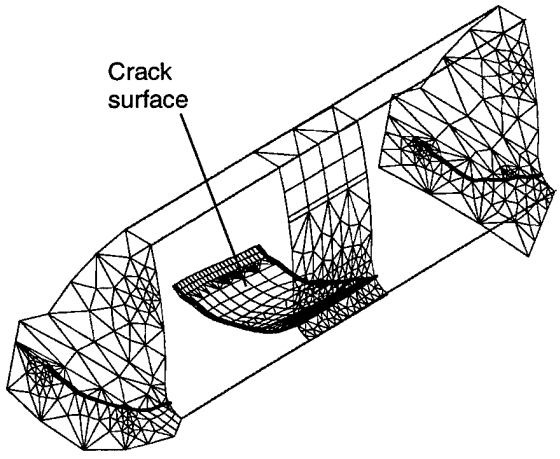

Figure 11. Exploded gear tooth view of predicted crack growth after 15 steps.

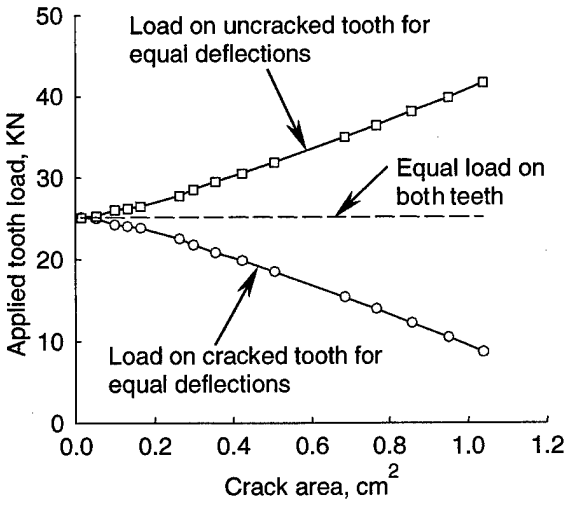

Figure 12. Calculated tooth loads for equal deflections.

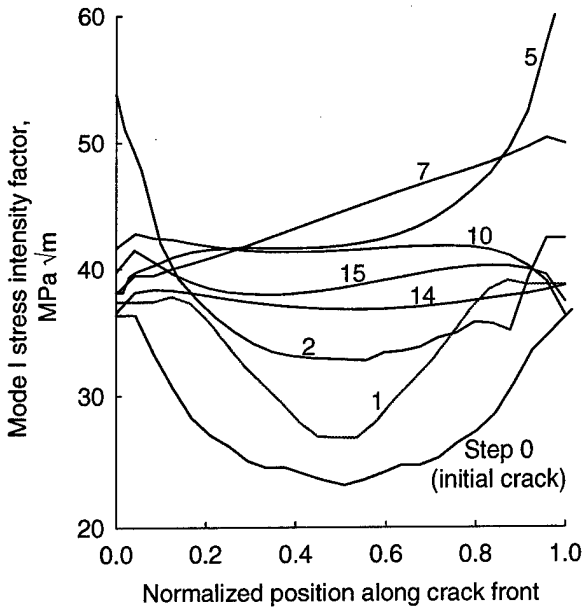

Figure 13. Mode I stress intensity factors for crack growth simulation study.

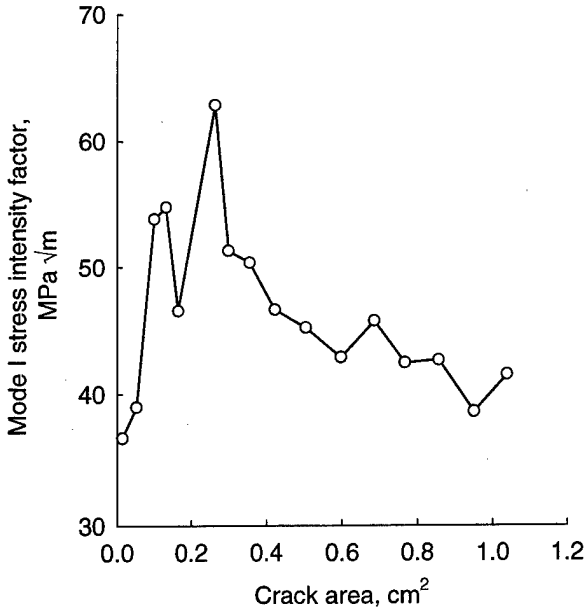

Figure 14. Maximum mode I stress intensity factors along crack front for all 15 steps of crack growth simulation study.

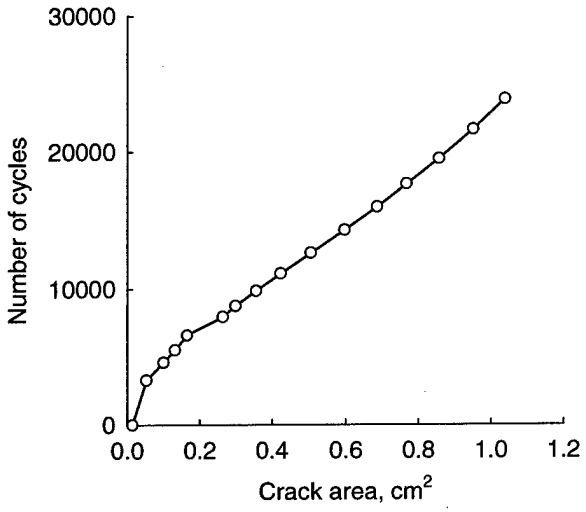

Figure 15. Gear tooth crack propagation life of the cracked tooth of a split-tooth design with an initial tooth fillet crack.

REPORT DOCUMENTATION PAGE

Form Approved
OMB No. 0704-0188

Public reporting burden for this collection of information is estimated to average 1 hour per response, including the time for reviewing instructions, searching existing data sources, gathering and maintaining the data needed, and completing and reviewing the collection of information. Send comments regarding this burden estimate or any other aspect of this collection of information, including suggestions for reducing this burden, to Washington Headquarters Services, Directorate for Information Operations and Reports, 1215 Jefferson Davis Highway, Suite 1204, Arlington, VA 22202-4302, and to the Office of Management and Budget, Paperwork Reduction Project (0704-0188), Washington, DC 20503.

1. AGENCY USE ONLY (*Leave blank*)	2. REPORT DATE	3. REPORT TYPE AND DATES COVERED
	December 1998	Technical Memorandum

4. TITLE AND SUBTITLE

Three–Dimensional Gear Crack Propagation Studies

5. FUNDING NUMBERS

WU–581–30–13–00
1L162211A47A

6. AUTHOR(S)

David G. Lewicki, Ashok D. Sane, Raymond J. Drago, and Paul A. Wawrzynek

7. PERFORMING ORGANIZATION NAME(S) AND ADDRESS(ES)

NASA Lewis Research Center
Cleveland, Ohio 44135–3191
and
U.S. Army Research Laboratory
Cleveland, Ohio 44135–3191

8. PERFORMING ORGANIZATION REPORT NUMBER

E–11436

9. SPONSORING/MONITORING AGENCY NAME(S) AND ADDRESS(ES)

National Aeronautics and Space Administration
Washington, DC 20546–0001
and
U.S. Army Research Laboratory
Adelphi, Maryland 20783–1145

10. SPONSORING/MONITORING AGENCY REPORT NUMBER

NASA TM—1998-208827
ARL–TR–1833

11. SUPPLEMENTARY NOTES

Prepared for the Fourth World Congress on Gearing and Power Transmission sponsored by the Institut des Engrenages et des Transmissions, Paris, France, March 16–18, 1999. David G. Lewicki, U.S. Army Research Laboratory, NASA Lewis Research Center; Ashok D. Sane and Raymond J. Drago, Boeing Defense and Space Group, Philadelphia, Pennsylvania 19142; Paul A. Wawrzynek, Cornell University, Ithaca, New York 14853. Responsible person, David G. Lewicki, organization code 0300, (216) 433-3970.

12a. DISTRIBUTION/AVAILABILITY STATEMENT

Unclassified - Unlimited
Subject Category: 37 Distribution: Nonstandard

This publication is available from the NASA Center for AeroSpace Information, (301) 621–0390.

12b. DISTRIBUTION CODE

13. ABSTRACT ***(Maximum 200 words)***

Three-dimensional crack growth simulation was performed on a split-tooth gear design using boundary element modeling and linear elastic fracture mechanics. Initial cracks in the fillet of the teeth produced stress intensity factors of greater magnitude (and thus, greater crack growth rates) than those in the root or groove areas of the teeth. Crack growth simulation was performed on a case study to evaluate crack propagation paths. Tooth fracture was predicted from the crack growth simulation for an initial crack in the tooth fillet region. Tooth loads on the uncracked mesh of the split-tooth design were up to five times greater than those on the cracked mesh if equal deflections of the cracked and uncracked teeth were considered. Predicted crack shapes as well as crack propagation life are presented based on calculated stress intensity factors, mixed-mode crack propagation trajectory theories, and fatigue crack growth theories.

14. SUBJECT TERMS

Gears; Crack propagation; Stress intensity factors; Safety; Boundary elements methods

15. NUMBER OF PAGES

16

16. PRICE CODE

A03

17. SECURITY CLASSIFICATION OF REPORT	18. SECURITY CLASSIFICATION OF THIS PAGE	19. SECURITY CLASSIFICATION OF ABSTRACT	20. LIMITATION OF ABSTRACT
Unclassified	Unclassified	Unclassified	